ELSEVIER

Journal of Molecular Catalysis A: Chemical 180 (2002) 161–168

JOURNAL OF MOLECULAR CATALYSIS A: CHEMICAL

www.elsevier.com/locate/molcata

Zirconia supported La, Co oxides and $LaCoO_3$ perovskite: structural characterization and catalytic CO oxidation

S. Colonna [a], S. De Rossi [b], M. Faticanti [b], I. Pettiti [b], P. Porta [b,*]

[a] *Istituto di Struttura della Materia, CNR, Via Fosso del Cavaliere 100, 00133 Rome, Italy*

[b] *Centro di Studio, Struttura e Attività Catalitica di Sistemi di Ossidi', CNR, c/o Dipartimento di Chimica, Università degli Studi di Roma, La Sapienza', Piazzale Aldo Moro 5, 00185 Rome, Italy*

Received 19 July 2001; received in revised form 12 October 2001; accepted 12 October 2001

Abstract

ZrO_2-supported La, Co oxide catalysts with different La, Co loading (2, 6, 8, 12 and 16 wt.% as $LaCoO_3$) were prepared by impregnation of tetragonal ZrO_2 with equimolar amounts of La and Co citrate precursors and calcination at 1073 K. The catalysts were characterized by X-ray diffraction (XRD), X-ray absorption spectroscopy (XAS), and BET specific surface area determination. Catalytic CO oxidation was performed at 298–800 K. XRD revealed the presence of tetragonal zirconia with traces of the monoclinic phase. $LaCoO_3$ perovskite was also detected for loading higher than 6%. XAS experiments suggested that at high loading $LaCoO_3$ and Co_3O_4 were formed, while at low loading, La, Co oxide species interacting with support, and hard to be structurally defined, prevailed. The catalysis study evidenced that the catalytic activity was due to segregated and highly dispersed cobalt oxide species.

Keywords: Zirconia-supported La; Co perovskites; CO oxidation

1. Introduction

Oxides with perovskite structure (ABO_3) and containing transition metal ions have attracted considerable interest for many years in the field of material science and heterogeneous catalysis [1–3]. A great variety of metal ions can be introduced in the perovskite structure provided that their ionic radii fit the sizes of the 12 coordinated A and octahedral B sites, e.g. $r_A > 0.90$ Å and $r_B > 0.51$ Å. Therefore, the ABO_3 perovskite lattice can be considered an ideal host matrix for many transition or nontransition metal ions.

One of the main drawbacks of the perovskites in catalytic investigations is their very low surface area (some $m^2\,g^{-1}$) when they are prepared by solid state reaction of the oxide precursors at high temperature [4,5]. Although, a method based on citrates precursors [6,7] allows the production of perovskites even with a few tens ($m^2\,g^{-1}$) of specific surface area after calcination at 1073 K [8–11], rapid sintering at higher temperatures cannot be avoided. We tried to extend the interface between the active material and gas phase by dispersing the perovskite components on a suitable support. In this respect zirconia seems to be a good choice because the interaction with the active phase is generally not strong enough as to favor bonds formation of the various oxides with the support therefore preventing the formation of the active compound and not so weak to cause the aggregation of

* Corresponding author. Tel.: +39-6-4991-3378; fax: +39-6-490-324.
E-mail address: piero.porta@uniroma1.it (P. Porta).

1381-1169/02/$ – see front matter
PII: S1381-1169(01)00422-8

the active components in large particles with loss of exposed surface area. Note that the specific activity of supported $LaCoO_3$ and $La_{0.8}Sr_{0.2}CoO_3$ perovskites in the oxidation of propane was found to be significantly enhanced only through the dispersion of a few layers on ZrO_2 [12,13].

In a previous paper devoted to La, Mn oxide systems supported on ZrO_2 [14] we observed that at low loading metal oxides were dispersed on the surface with low catalytic activity. Samples with high loading evidenced the presence of perovskite-type species and showed higher activity for both methane combustion and CO oxidation.

It was then interesting to study the analogous La, Co oxide systems supported on ZrO_2 in order to investigate the nature of the species formed at various loadings and study the catalytic behavior towards CO oxidation. In this paper we report the results of this investigation.

2. Experimental

La, Co oxides/ZrO_2 catalysts with different La–Co loading (hereafter designated as ZLaCo with the number after the label indicating the nominal perovskite content: 2, 6, 8, 12 and 16 wt.%) were prepared by impregnation of tetragonal ZrO_2 with equimolar amounts of citrate precursors.

Tetragonal ZrO_2 with a large surface area was prepared by the method of Chuah et al. [15]. An aqueous solution of 0.075 M $ZrOCl_2$ was added, drop wise (1 ml min^{-1}) and under magnetic stirring, to a 5 M NH_4OH solution. The hydrous zirconia, after digestion in its mother solution at 373 K for 48 h, was filtered, washed with water until the $AgNO_3$ test for Cl^- detection gave no opalescence in the washing solution, then dried in a furnace overnight at 383 K and finally calcined at 1073 K for 5 h (raising slowly the temperature by 1 K min^{-1}).

The dispersion of La, Co oxides on the ZrO_2 support was performed by the citrate method [6–11]. Two solutions were added to a weighted amount of ZrO_2: an aqueous solution of citric acid was added first and subsequently a solution containing $La(NO_3)_3$ and $Co(NO_3)_2$ in 1:1 proportions. The molar ratio between the citric acid and the overall metal nitrates was fixed at 1. The resulting solution was kept at 383 K until dryness and the samples, after grinding, were calcined at 1073 K for 5 h. For comparison, unsupported $LaCoO_3$ was also prepared by the citrate method as reported in [9].

BET surface area of samples (SA, $m^2\,g^{-1}$) was evaluated by nitrogen adsorption at 77 K in a vacuum glass apparatus. Phase analysis was performed by X-ray powder diffraction using a Philips PW 1029 diffractometer with Ni-filtered Cu Kα radiation. Spectra were recorded in a 2θ range from 20° to 60°.

X-ray absorption spectroscopy (XAS) measurements at the La and Co K-edges were done for ZLaCo-2, ZLaCo-6 and ZLaCo-12 materials, and for $LaCoO_3$, Co_3O_4 and La_2O_3 as reference samples. These measurements were done at the beam line GILDA, ESRF, Grenoble (France) in fluorescence detection for the catalysts samples and in transmission mode for the reference compounds. During the data collection the samples were held at the liquid nitrogen temperature. The beam line monochromator was equipped with two Si(3 1 1) crystals for Co K-edge measurements and two Si(5 1 1) crystals for La K-edge measurements. Powder samples were deposited on millipore membranes or mixed to an appropriate amount of boron nitride (BN) and pressed into pellets. The XANES part of the experimental signal was obtained by subtracting a linear pre-edge and normalizing to one in correspondence of the first EXAFS oscillation. The EXAFS analysis was performed by using the complete FEFF8 package [16]. Fourier transforms (FTs) for the signal $k^2\chi(k)$ were calculated in the range $2.5 < k < 11\,Å^{-1}$ by using a Kaiser window. Structural information was obtained by fitting the FT(R) function in the 1.0–4.0 Å range (1.0–4.3 Å for the ZLaCo-12 sample, on La K-edge).

The CO oxidation with O_2 was studied in a flow system in the range from room temperature to 800 K using 0.5 g of catalyst supported on a silica fritted disk internal to a silica reactor vertically positioned in a tubular electrical heater.

A Ni–NiCr thermocouple was positioned in the middle of the catalyst bed. An ASCON XS proportional programmer powered the heater and was set to produce a linear temperature ramp of 1 K min^{-1} from 298 to 800 K.

The composition and the total flow rate of the reactants were adjusted to 1% CO, 20% O_2, balance He by volume and 100 cm^3 STP min^{-1}, employing

independent electronic flow controllers MKS model 1259 driven by an MKS unit model 147. The space velocity resulted 12 000 cm^3 STP h^{-1} g^{-1}.

At time intervals of 20 min, that is every 20 K, a sample of 1 cm^3 of effluent from the reactor was sampled and analyzed by gas-chromatography, using an Alltech CTR 1 column made of two coaxial columns held at RT. The inner column was packed with Porapak®, whereas the outer one contained a molecular sieve packing. A thermal conductivity detector was used to reveal CO_2, O_2 and residual CO. The mass balance with respect to carbon was 100±2%. Before each run a standard pretreatment at 773 K with oxygen in flow at 100 cm^3 STP min^{-1} for 0.5 h was carried out.

3. Results and discussion

Phase analysis, performed by X-ray powder diffraction, showed that up to 6% loading no other phase, except tetragonal zirconia (with only traces of the monoclinic phase), was revealed. Fig. 1 shows that in the ZLaCo-8, ZLaCo-12 and ZLaCo-16 samples, in addition to the ZrO_2 X-ray diffraction (XRD) pattern, small peaks are visible. Their intensity increases at the increase of La–Co loading, their position corresponding to that of the strongest peaks of $LaCoO_3$ perovskite.

Preparation method leads to the stabilization of ZrO_2 in its tetragonal phase characterized by a BET surface area of 82 m^2 g^{-1} even after 5 h calcination at 1073 K, making it suitable as catalyst support. Dispersion of active components and following calcination step yielded final surface areas of ZLaCo samples in the range 60–80 m^2 g^{-1}.

First derivatives of the XANES spectra are shown in Fig. 2. More evidently at high cobalt loading, the first derivative profiles show some structures at lower energy with respect to the maximum that are typical for Co_3O_4. It seems that, with increasing Co content,

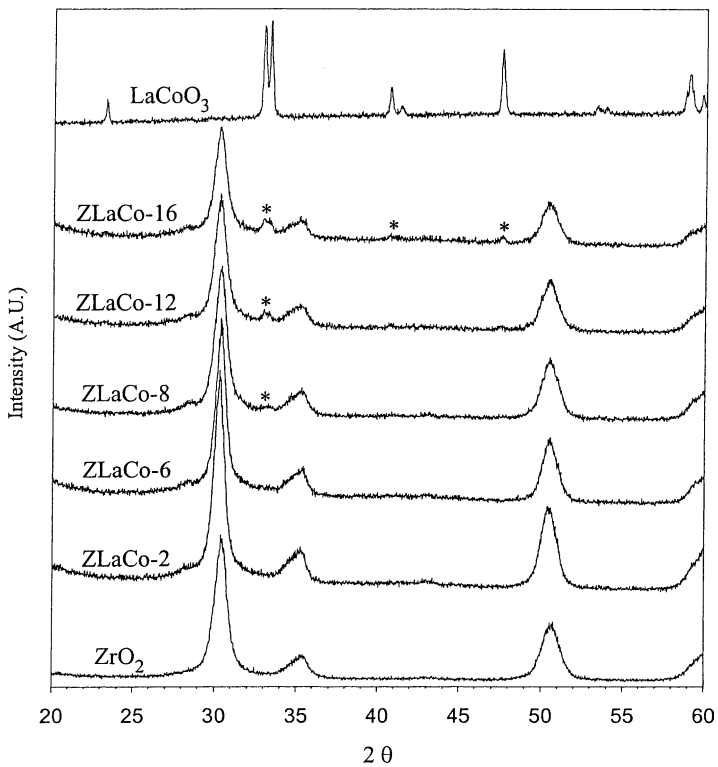

Fig. 1. XRD patterns of ZrO_2, $LaCoO_3$ and ZLaCo catalysts. Asterisks indicate the most intense X-ray lines of $LaCoO_3$.

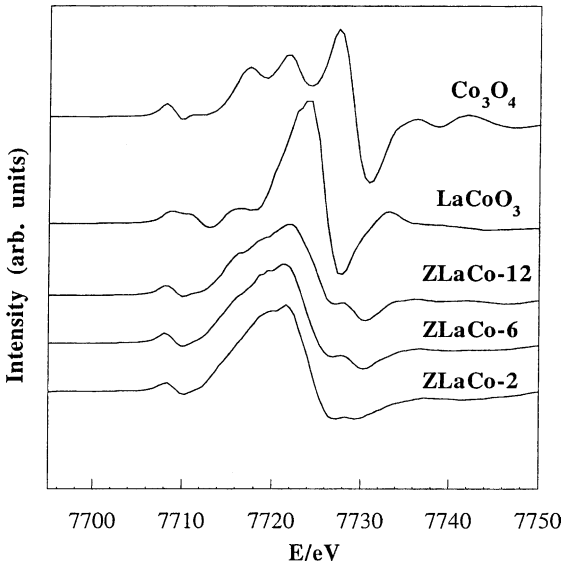

Fig. 2. First derivatives of the Co K-edge XANES spectra for Co_3O_4, $LaCoO_3$ and ZLaCo supported systems.

cobalt oxide can be formed on the surface of the zirconia support, thus inhibiting the formation of the perovskite phase.

This hypothesis was confirmed by the EXAFS analysis. The fine structure of the samples was investigated at the Co K-edge (for ZLaCo-2, ZLaCo-6 and ZLaCo-12) and at the La K-edge (for ZLaCo-2 and ZLaCo-12).

Fig. 3 shows the FTs (solid lines) of the EXAFS signals collected at the Co K-edge for the samples compared to pure $LaCoO_3$ (upper panel). In the same figure the dotted lines represent the fits obtained by using the standard EXAFS formula. For $LaCoO_3$, the FT presents a first shell peak at about 1.8 Å, second shell peaks in the 2.0–4.0 Å range due to both Co–Co and Co–La contributions and a broad, not very intense, peak at about 5.0 Å. As to the supported samples, the FTs show a broadening of the first shell peak, particularly evident for the ZLaCo-6 sample, revealing heterogeneity of the Co–O contributions due to surface disorder probably related to the presence of different cobalt-containing oxide phases. Moreover, for the FTs, the greatest differences appear in the 2.0–5.0 Å range. The ZLaCo-2 material shows the most intense second shell peak at about 3.2 Å, while for the ZLaCo-6 and ZLaCo-12 samples the most relevant second shell

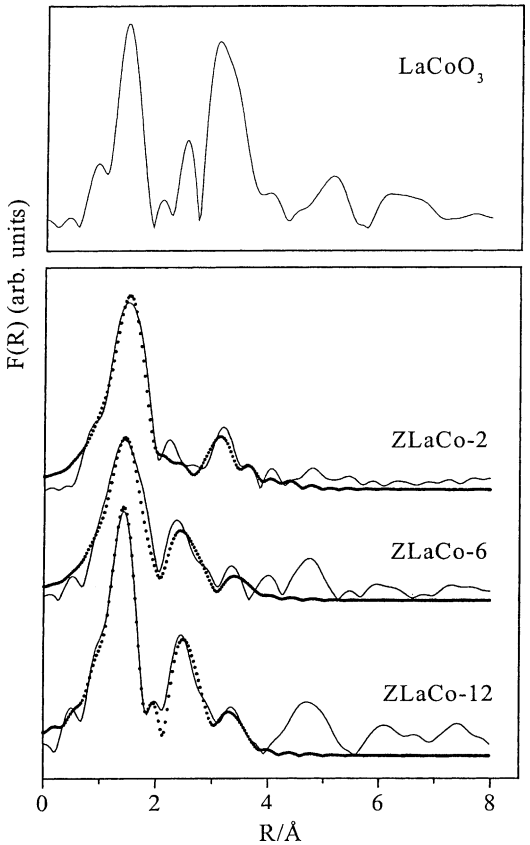

Fig. 3. Co K-edge: FTs of the $k^2\chi(k)$ signals for the ZLaCo-2, ZLaCo-6 and ZLaCo-12 samples compared to pure $LaCoO_3$. The continuous line represents the experimental data and the dots are the fit profiles.

peak is centered at about 2.5 Å. In addition, the Co richer samples present a broadened third shell peak at about 4.8 Å, a distance that is slightly shorter than that of the broad peak appearing in the FT of pure $LaCoO_3$.

The FTs of the $LaCoO_3$ and Co_3O_4 reference compounds were fitted by using the crystallographic bond distances data [17,18], and leaving free the E_0 shift, the S_0^2 term and the Debye–Waller factors. In the fitting procedure of the ZLaCo samples two Co–O contributions were used to reproduce the near neighbors coordination. The second shell structures were fitted using both Co–Co and Co–La contributions. Debye–Waller, E_0 and S_0^2 parameters were fixed to the value obtained from the fit of the reference compounds. The coordination numbers (N) and bond distances (R) were left to vary in the fit. The Debye–Waller factors were

Table 1
Coordination numbers (N) and bond distances (R) obtained from EXAFS data for ZLaCo and $LaCoO_3$ samples

Co K-edge	Co–O	Co–O	Co–Co	Co–Co	Co–La	Co–La	Co–Co
ZLaCo-2							
$N \pm 0.5$	2.1	2.4	–	–	0.5	4.2	3.8
R (Å) ± 0.02	1.96	2.09	–	–	3.62	3.80	3.93
ZLaCo-6							
$N \pm 0.5$	2.0	2.1	0.8	0.1	0.9	–	–
R (Å) ± 0.02	1.92	2.07	2.91	3.34	3.64	–	–
ZLaCo-12							
$N \pm 0.5$	3.4	1.4	1.4	0.3	1.0	–	–
R (Å) ± 0.02	1.92	2.08	2.93	3.25	3.65	–	–
$LaCoO_3$							
N	6.0	–	–	–	2.0	6.0	6.0
R (Å)	1.93	–	–	–	3.25	3.31	3.81
La K-edge	La–O	La–O	La–O	La–Co	La–Co	La–La	La–La
ZLaCo-2							
$N \pm 0.5$	5.7	4.5	3.2	2.1	1.8	1.2	–
R (Å) ± 0.02	2.49	2.60	3.27	3.51	3.77	4.01	–
ZLaCo-12							
$N \pm 0.5$	3.0	6.2	0.5	5.3	1.8	1.7	2.5
R (Å) ± 0.02	2.34	2.54	3.63	3.34	3.51	3.84	4.29
$LaCoO_3$							
N	3.0	6.0	3.0	2.0	6.0	6.0	–
R (Å)	2.43	2.69	3.00	3.25	3.31	3.81	–

fixed to avoid the strong correlation with the coordination numbers. The fit results, reported in Table 1, reveal that in the ZLaCo-2 sample a La–Co mixed oxide phase dispersed on the zirconia surface probably occurred, whose structure is not equal to perovskite. In fact, the fitted Co–Co (3.93 Å) and Co–La (3.62 and 3.80 Å) bond distances are longer than those expected for the $LaCoO_3$ perovskite (Co–Co: 3.81 Å and Co–La: 3.31 Å, from crystallographic data [18]). In the samples with higher Co loading (ZLaCo-6 and ZLaCo-12), the prevailing formation of dispersed Co_3O_4-like species together with some well dispersed La–Co mixed oxide was evidenced. In fact, the fitted Co–Co bond distances (in the 2.91–2.93 and 3.25–3.34 Å ranges, Table 1) resemble those of Co_3O_4 (2.85 and 3.35 Å, from crystallographic data [19]) and a single Co–La contribution was found with a bond distance at about 3.65 Å and a very low coordination number ($N \sim 1$) for both samples. In all the fits, the reduced coordination numbers, found for all the coordination shells, indicate a disorder on the surface of the support, and/or the presence of small crystallites.

In order to verify these evidences, the EXAFS analysis was also performed on La K-edge for the ZLaCo-2 and ZLaCo-12 catalysts. Fig. 4 shows the FTs for these samples compared to that of $LaCoO_3$ (upper panel). As in Fig. 3 the solid lines are the experimental data and the dotted ones represent the fits. In the 1.0–4.3 Å range, the FTs of the ZLaCo samples show three most intense structures, the first is a double peak in the range 1.0–2.2 Å, then a single peak at about 2.6 Å (much more intense for the ZLaCo-12 compound) and a double peak in the 2.8–4.3 Å range. These structures are shifted to higher distances in the most concentrated ZLaCo-12 sample. Fits were performed using three La–O, two La–Co and one La–La contributions. For ZLaCo-12 a further La–La shell was added as really improving the quality of the fit. The Debye–Waller factors were fixed to the values obtained from the fits of the reference compounds. The results, reported in Table 1, confirm that, in the

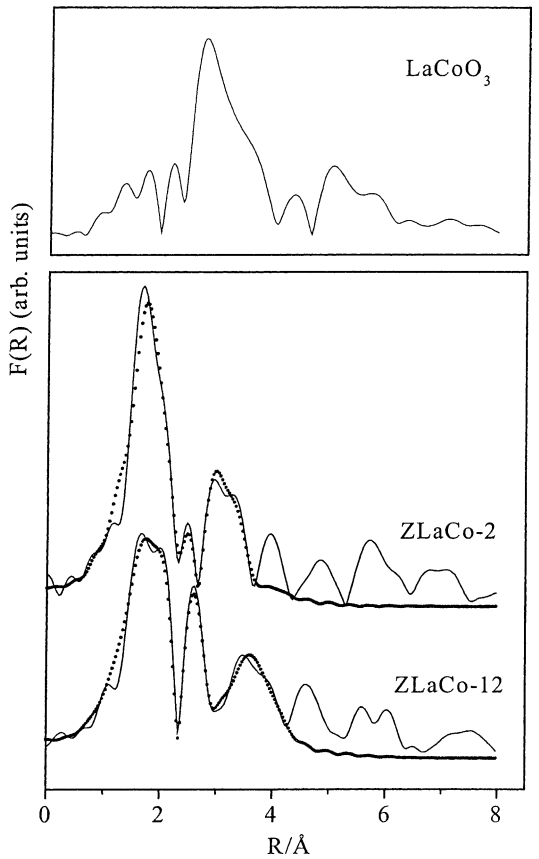

Fig. 4. La K-edge: FTs of the $k^2\chi(k)$ signals for the ZLaCo-2 and ZLaCo-12 samples compared to pure $LaCoO_3$. The continuous line represents the experimental data and the dots are the fit profiles.

most diluted sample, a dispersed La–Co mixed oxide phase was probably formed on the surface of the zirconia support. The two shorter La–O bond distances are close to those of $LaCoO_3$, but all the other distances are really longer, thus testifying against the formation of a perovskite-type structure. Low values of the coordination numbers for the La–Co and La–La shells should also confirm a disorder on the surface of the support, and/or the presence of small crystallites. For the ZLaCo-12 sample, the situation seems to be different and more complicated. In fact, the fit reveals the presence of a very long La–O bond distance at 3.63 Å, with low coordination numbers ($N = 0.5$), which could be attributed to some well dispersed lanthanum oxide species (in La_2O_3, La–O = 3.67 Å, from crystallographic data [19]). Moreover, one of the two fitted La–Co bond distances, 3.34 Å, results to be similar to the distance in $LaCoO_3$ (3.31 Å) but the other one, 3.51 Å, is still too long for attributing properly to a perovskite structure. Also for the two fitted La–La bond distances, the first, 3.84 Å, is similar to $LaCoO_3$ (3.81 Å), the second one, 4.29 Å, is too long for perovskite. So, the most reliable hypothesis for the ZLaCo-12 catalyst is the formation of different phases on the surface of the zirconia support: a mixed La–Co oxide whose structure is evolving towards the perovskite and some well dispersed single lanthanum and cobalt oxides. Finally, in the ZLaCo-12 sample the total coordination numbers of the La–Co and La–La contributions are enhanced with respect to the most diluted ZLaCo-2 sample, revealing a greater aggregation of the La–Co mixed oxide on the surface of the support at higher loading.

ZLaCo catalysts show activity in CO oxidation already at room temperature, whereas ZrO_2 is active only above 550 K. In particular, the initial CO conversion was 100% for ZLaCo-8, ZLaCo-12, ZLaCo-16 and for a sample of Co_3O_4 examined for reference, while the conversion was 90, 78, and 10%, for ZLaCo-6, ZLaCo-2 and $LaCoO_3$, respectively (Fig. 5). Hence, a study of the dependence of the activity on the temperature is possible only for the support ZrO_2 and the perovskite $LaCoO_3$. The results

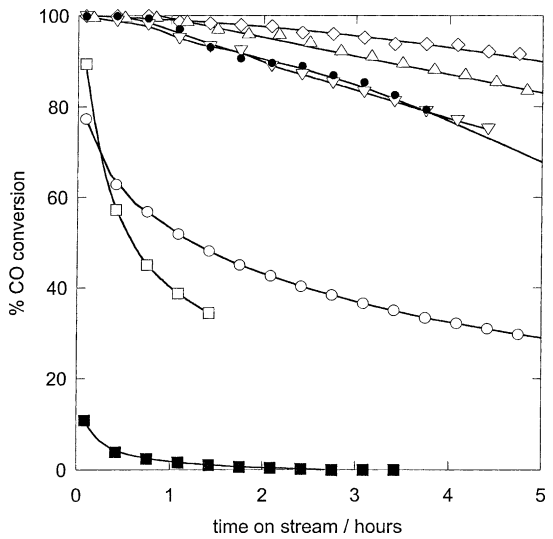

Fig. 5. Percentage of CO conversion at 298 K on: (○) ZLaCo-2; (□) ZLaCo-6; (▽) ZLaCo-8; (◇) ZLaCo-12; (△) ZLaCo-16; (◆) $LaCoO_3$; (●) Co_3O_4.

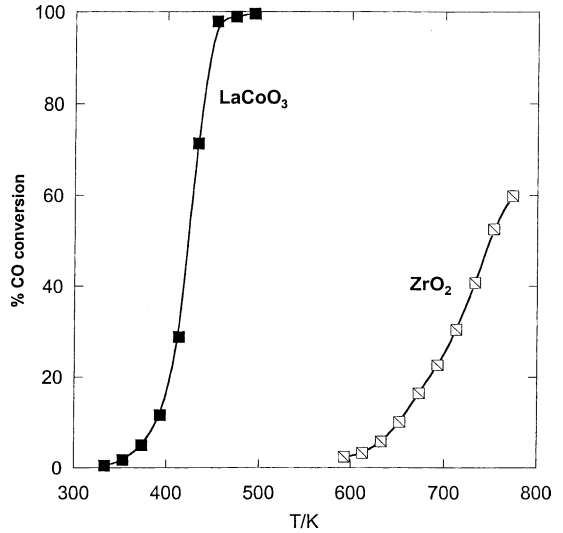

Fig. 6. Percentage of CO conversion vs. temperature for $LaCoO_3$ and ZrO_2.

for these latter samples are shown in Fig. 6, where, it can be seen that 100% conversion is achieved for $LaCoO_3$ at 500 K, at which temperature ZrO_2 is still inactive. From the Arrhenius plot (Fig. 7), apparent activation energy values of 64 and 84 kJ mol^{-1} can be derived for $LaCoO_3$ and ZrO_2, respectively.

All the catalysts, except ZrO_2, showed a continuous deactivation with time on stream in isothermal runs at 298 K even after many hours (Fig. 8). The deactivation is most probably due to a strong chemisorption of the product, possibly under form of surface carbonates, which do not decompose at room temperature and progressively block the active sites. Other reasons for the deactivation as, for instance, formation of carbon residues are less probable due to the presence of excess oxygen in the feed.

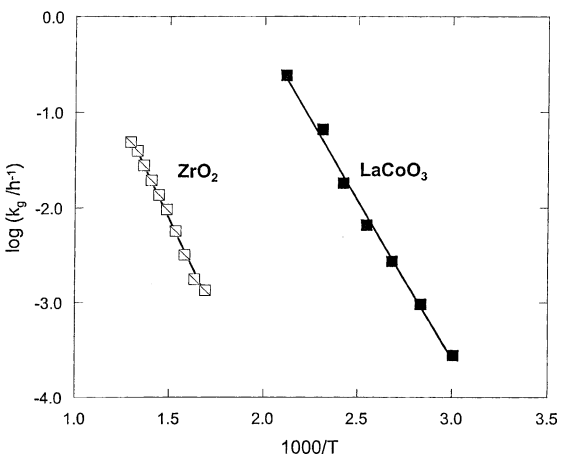

Fig. 7. Arrhenius plots for $LaCoO_3$ and ZrO_2.

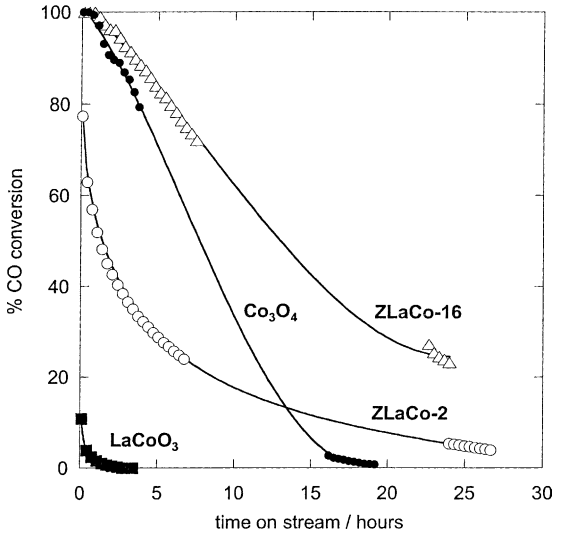

Fig. 8. Deactivation with time on stream in isothermal runs at 298 K for Co_3O_4, $LaCoO_3$, and ZLaCo-2, ZLaCo-16 supported systems.

By following the deactivation curves it is possible to establish a rank for the activity of the various catalysts, that is: ZLaCo-16 ≅ ZLaCo-12 > ZLaCo-8 > ZLaCo-6 ≅ ZLaCo-2 (Fig. 5). Thus, the higher the cobalt content the higher the activity in CO oxidation. This finding together with the high activity of Co_3O_4, compared with the low activity of $LaCoO_3$ perovskite and the lack of activity at room temperature of the zirconia support, strongly suggests that on all the supported systems the activity for CO oxidation is due to the presence of segregated and highly dispersed Co_3O_4, which escape detection by XRD. The $LaCoO_3$ perovskite, when present, only poorly contribute to the catalytic activity.

4. Conclusions

XRD analysis for the zirconia-supported samples shows only the tetragonal zirconia phase with traces of monoclinic zirconia up to the loading of 6%. At higher loading XRD also shows the presence of the perovskite

$LaCoO_3$ phase. XAS analysis confirms the formation of $LaCoO_3$ together with cobalt oxide species dispersed on zirconia at high La–Co loading, whereas at low loading the presence of disordered oxide species strongly interacting with support is suggested.

The ZrO_2 support does not contribute to the activity of supported sample due to its very low activity. All the ZLaCo and $LaCoO_3$ are active at room temperature. However, they undergo deactivation with time on stream due to the strong chemisorption of the product most probably under form of carbonates, which do not decompose at room temperature. The activity of the supported samples is related to the presence of dispersed Co_3O_4, which escape detection by XRD. The contribution to the activity of the $LaCoO_3$ perovskite when present is probably low.

References

[1] L.G. Tejuca, J.L.G. Fierro (Eds.), Properties and Applications of Perovskite-type Oxides, Marcel Dekker, New York, 1993.
[2] R.E. Newman, A. Navrotsky, D.J. Weidner (Eds.), Structure–Property Relationship in Perovskite Electroceramics. Perovskite: A Structure of Great Interest to Geophysics and Material Science, American Geophysical Union, Washington, DC, 1989, p. 66.
[3] R.J.H. Voorhoeve, Advanced Materials in Catalysis, Academic Press, New York, 1977, p. 129.
[4] H. Arai, T. Yamada, K. Eguchi, T. Seiyama, Appl. Catal. 26 (1986) 265.
[5] L.G. Tejuca, J.L.G. Fierro, J.M.D. Tascón, Adv. Catal. 36 (1989) 237.
[6] Belgium Patent 735,476 (1969).
[7] B. Delmon, W.H. Droguest, J. Fuhn (Eds.), Proceedings of the Second International Conference on Fine Particles, The Electrochemical Society, 1973, p. 242.
[8] L. Lisi, G. Bagnasco, P. Ciambelli, S. De Rossi, P. Porta, G. Russo, M. Turco, J. Solid State Chem. 146 (1999) 176.
[9] P. Porta, S. De Rossi, M. Faticanti, G. Minelli, I. Pettiti, L. Lisi, M. Turco, J. Solid State Chem. 146 (1999) 291.
[10] P. Ciambelli, S. Cimino, G. De Rossi, M. Faticanti, L. Lisi, G. Minelli, I. Pettiti, P. Porta, G. Russo, M. Turco, Appl. Catal. B 24 (2000) 243.
[11] P. Ciambelli, S. Cimino, S. De Rossi, L. Lisi, G. Minelli, P. Porta, G. Russo, Appl. Catal. B 24 (2001) 243.
[12] H. Fuji, N. Mizuno, M. Misono, Chem. Lett. 2147 (1987).
[13] N. Mizuno, H. Fuji, H. Igarashi, M. Misono, J. Am. Chem. Soc. 114 (1992) 7151.
[14] S. Cimino, S. Colonna, S. De Rossi, M. Faticanti, L. Lisi, I. Pettiti, P. Porta, J. Catal., in press.
[15] G.K. Chuah, S. Janice, S.A. Cheong, Appl. Catal. A 145 (1996) 267.
[16] A.L. Ankudinov, B. Ravel, J.J. Rehr, S.D. Conradson, Phys. Rev. B 58 (1998) 7565.
[17] G. Thornton, B.C. Tofield, A.W. Hewat, J. Solid State Chem. 61 (1986) 301.
[18] R.J. Hill, J.R. Craig, G.V. Gibbs, Phys. Chem. Miner. 4 (1979) 317.
[19] R.W.G. Wyckoff, Crystal Structures, Vol. 2, 2nd Edition, Interscience/Wiley, New York, 1964, p. 1.